STOCHASTIC BOUNDARY PLASMA IN TOKAMAKS WITH RESONANT MAGNETIC PERTURBATIONS

Y. Liang

Forschungszentrum Jülich GmbH, Institut für Energie- und Klimaforschung - Plasmaphysik, 52425 Jülich, Germany

August 10, 2015

ABSTRACT

Experimental results from different devices demonstrate that magnetic topology plays a key role in plasma confinement, edge MHD stability, and interactions between the plasma and the first wall, particularly with the divertor. Recently, three-dimensional (3D) magnetic topology effects, which are associated with stochastic boundary plasma physics, form one of the hottest topics in fusion research today, and understanding them is essential for the success of future fusion devices. In this paper, an overview of the physics understanding of the formation first of 3D magnetic topology and then of a stochastic layer, and its effects on the edge and divertor transport and on MHD stability in tokamak plasmas will be presented. In addition, comparing the advantages and disadvantages of 2D and 3D magnetic topology effects in magnetic confinement fusion will be discussed.

I. INTRODUCTION

On the basis of the fusion reseach achievements of the past half century, it is foreseen that a steady state operation of ITER [1] and future fusion power plants, e.g. DEMO, will require the resolution of plasma wall interaction, in which a tolerable plasma exhaust, including steady state and transient heat and particle fluxes on plasma-facing components, is controlled reliably by one or more mechanisms at high power densities.

A. Problem of transient plasma wall interaction

The standard tokamak H-mode [2] is foreseen as the baseline operating scenario of a future fusion machine, e.g. ITER. However, the steep plasma pressure gradient and associated increased current density at the edge pedestal could exceed a threshold value for driving magnetohydrodynamic (MHD) instabilities referred to as Edge Localized Modes (ELMs). Using results from various current devices, an extrapolation of the heat and particles deposited on the wall components has been carried out for ITER. Since the exact physics and scaling is unknown, the predicted ELM energy loss ranges from $\sim$ 5 to $22MJ$[4]. It is expected that approximately half of this energy will reach the wall and be deposited over a region of $\sim 1m^2$, known as the wetted area. Thus, the surface energy density is suggested to be 2.5 to $11MJm^{-2}$ which is $\sim$ 5 to 20 times higher than acceptable for the planned first wall components, primarily made of tungsten or carbon fibre composites, which can receive a maximum of $0.5MJm^{-2}$. Therefore, it is important to find mitigation/suppression solutions for ELMs.

B. Problem of stationary plasma-wall interaction

In a fusion reactor, a significant amount of heating power, which is mainly from auxiliary heating and energetic α particles produced in the D-T burning plasmas, has to be continuously exhausted through radiation or deposited directly on the plasma facing components during long-pulse or steady-state operation. Since the transport along field lines is several orders of magnitude higher than the cross field transport, this results a very rapid decay of the profiles inside the scrape-off layer (SOL) which causes a thin power deposition width,λ_q.

$$\lambda_q \approx \pi q R \sqrt{\frac{\chi_\parallel}{\chi_\perp}}, \tag{1}$$

Here, R is the major radius of the tokamak, q is the safety factor at the edge, $\chi_\parallel$ and $\chi_\perp$ are the energy diffusion coefficients in the direction parallel and perpendicular to the field lines, respectively.

Based on the present experimental scaling[3], λ_q is expected to be less than $1mm$, and then the parallel heat flux may approach $1GWm^{-2}$ for ITER. This obviously exceeds the engineering capability for any plasma-facing component. Therefore, it is necessary both to decrease the power conducted and convected to the edge by enhancing exhaust through non-magnetically confined particles (neutral atoms or photons) and also to increase the λ_q by controlling the edge plasma transport.

C. Stochasticity in Fusion Plasmas

The success of the *stochastic ansatz* goes back to 1905, when Einstein published three fundamental papers, one of which was on Brownian motion

[5, 6], a simple continuous-time stochastic process in natural science. Nowadays, the term stochastic occurs in a wide variety of professional or academic fields to describe events or systems that are unpredictable due to the influence of a random variable. The theory of stochasticity has been further developed [7, 8, 9, 10, 11]. Recently, *stochastic transport* theory was developed for plasmas [12].

In a magnetically confined fusion device, resonant magnetic perturbations (RMPs) can tear the nested flux surfaces and generate magnetic islands. The width of the magnetic island is proportional to the square root of the perturbation field. By simply increasing the perturbation field, the island width can be increased. Due to the fixed distance between neighbouring islands, the island chains will grow and further overlap. Then, the field lines start to behave in a chaotic way and all closed flux surfaces between the two surfaces will be destroyed. A standard criterion of stochastization is the Chirikov parameter, σ_{ch}, which is the ratio of the island width to the radial distance between the neighbouring island-chains. When $\sigma_{ch} \geq 1$, the criterion indicates island overlapping [8]. The magnetic fields between these two surfaces are now called *stochastic* or *ergodic*. These two terms are used with almost the same meaning in the fusion community although there is some difference in their mathematical meanings. If the overlapping of island chains exists, the transport (radial) will be greatly enhanced and the pedestal gradient could be reduced.

Very recently, structure formation and transport in stochastic plasmas has been a topic of growing importance in many fields of plasma physics from astrophysics to fusion research. In particular, the investigation of the possibility of controlling the particle and heat transport by the formation of a stochastic boundary layer has been investigated on most large and medium-sized magnetic confinement fusion devices across the world [13]. A major result was discovering that large type-I ELMs in H-mode tokamak plasmas can be mitigated [14]or even suppressed [15] by RMPs. This discovery opens up a possible mechanism for suppressing large type-I ELMs in future fusion devices such as ITER. However, it is widely recognized that a more basic understanding of the plasma response to the RMPs is needed to extrapolate the results obtained in present experiments to future fusion devices.

D. Scope of this lecture

This lecture will address the topic of stochastic boundaries and focus on three-dimensional (3D) edge physics and applications of RMPs in tokamaks. However, this topic itself is not specific to the tokamak magnetic configuration. In both tokamaks and stellarators, stochastic magnetic fields can arise and influence the interplay between 3D magnetic topology and plasma confinement. Stellarator devices represent an inherent 3D challenge. They make use of the island divertor concept, and stochasticity and magnetic topology therefore play a fundamental role in their operation. With the extended operational regimes pioneered on the Large Helical Device (LHD), and with W7-X, attention has been directed towards the challenge of 3D plasma equlibria, transport and plasma-surface interactions.

In this lecture, the fundamental physics of the formation of a stochastic boundary layer by the application of RMPs will be described. The physics of stochastic boundary plasmas including the rotational screening effect, the plasma equilibrium effect on the magnetic topology, and stochastic plasma transport and its effects on plasma-wall interactions will be discussed. Finally, the application of RMPs for controlling pedestal profiles and stability will be presented.

II. FORMATION OF A STOCHASTIC BOUNDARY LAYER IN MAGNETICALLY CONFINED FUSION PLASMAS

A. Resonant magnetic perturbations

Magnetic perturbations which are resonant with field lines in the plasma are known as RMPs. The resonance condition is fulfilled when the inverse winding number of the field lines, in tokamak physics known as the safety-factor

$$q = \frac{1}{2\pi} \oint \frac{B_t}{R B_p ds}, \tag{2}$$

corresponds to the ratio of the applied poloidal m and toroidal n perturbation mode numbers: $q = \frac{m}{n}$. Here, R is the major radius of the torus, B_t and B_p the toroidal and poloidal magnetic field components, and ds the line element in the poloidal plane. The term RMP is mostly used if the perturbation is deliberately applied. In a magnetic confinement device, several resonance conditions are usually fulfilled due to the continuous q-profile. As will be seen below, the key resonant perturbations are those in the plasma boundary.

B. Methods of producing RMPs

A standard technique for producing such RMPs is the usage of either in-vessel or external coil systems with a certain geometry to apply the required poloidal and toroidal mode numbers. The main focus is often on low toroidal mode numbers, usually in the range of 1 to 4. Although the general idea is always the same, the design of such RMP coil systems differs greatly from device to device.

On JET, the error field correction coils (EFCCs), which are located outside of the vacuum vessel, as seen in figure 1, are used to apply RMPs. They were originally designed to correct the intrinsic error field of misaligned toroidal field coils. As a consequence of

the large distance between the coils and the plasma edge, a strong current of several tens of kA is required to achieve an adequate perturbation of the plasma edge using such EFCCs.

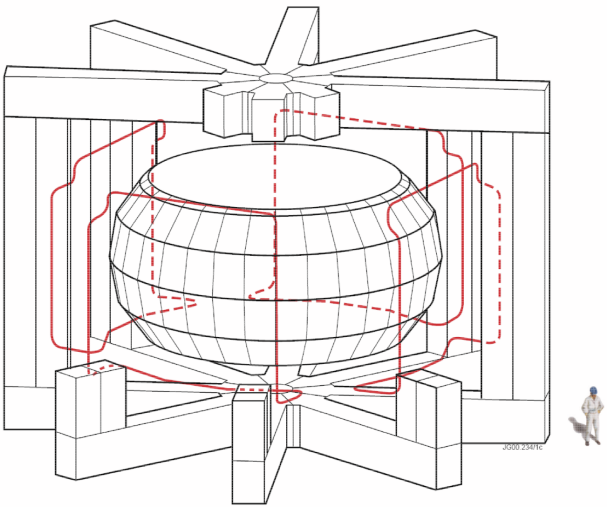

Figure 1: Perspective view of JET showing the 4 large error field correction coils mounted between the transformer limbs.

Depending on the wiring of the EFCCs, either $n = 1$ or $n = 2$ fields can be created [17]. The effective radial resonant magnetic perturbation amplitude, $|b_{res}^{r,eff}| = |B_{res}^{r,eff}/B_0|$, where $B_{res}^{r,eff}$ and B_0 are the radial resonant magnetic perturbation field and the on-axis toroidal magnetic field, respectively, calculated for $I_{EFCC} = 1kAt$ in $n = 2$ configuration, is shown in figure 2. $|b_{n=2}^{r,eff}|$ is the $n = 2$ effective radial resonant magnetic perturbation amplitude.

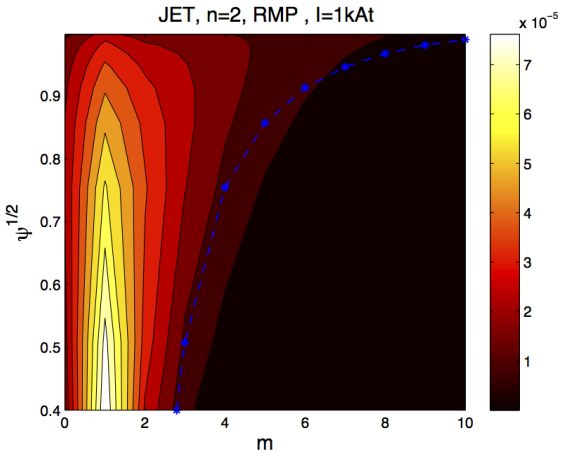

Figure 2: Radial component of the $n = 2$ helical mode spectrum with $I_{EFCC} = 1kAt$ using vacuum fields. Here, the x-axis is the poloidal mode number, m. The calculation is based on an equilibrium reconstruction for JET pulse #69557 at $20s$. Pitch resonant modes with $m = nq(\Psi)$ are shown by the blue dashed line.

Recently, the formation of helical current filaments flowing along field lines has been observed in the SOL during the application of lower hybrid waves (LHWs) on the Experimental Advanced Superconducting Tokamak (EAST) [18]. Magnetic perturbations induced by the currents flowing in these edge helical filament structures have been measured by a set of Mirnov coils during the modulation of LHWs. Because of the geometric effect of the LHW antenna, the perturbation fields induced by the HCFs are dominated by the $n = 1$ component. The magnetic perturbation spectrum calculated based on the experimental parameters indicates a good resonant feature, whereby the plasma edge resonant surfaces are well aligned on the ridge of the spectrum as seen in figure 3.

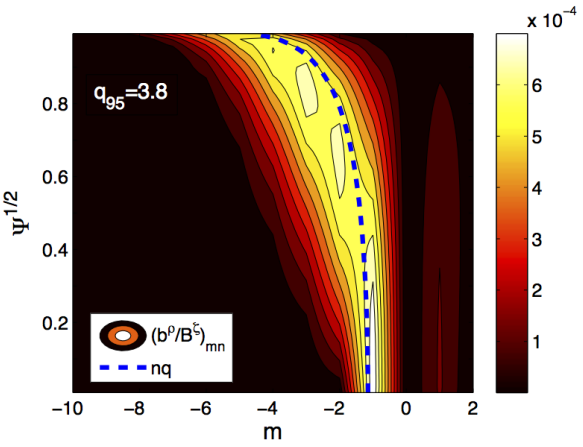

Figure 3: Radial component of the $n = 1$ helical mode spectrum calculated with $1kA$ HCF current. The calculation is based on an equilibrium reconstruction for a EAST pulse. Pitch resonant modes with $m = nq(\Psi)$ are shown by the blue dashed line.

C. 3D magnetic topology in tokamaks with RMPs

The application of RMPs results in the reorganization of the magnetic topology into a new equilibrium state. Resonances outside the plasma (in the SOL) cause an external kinking of the plasma; resonances inside the plasma lead to internal kinking and magnetic reconnection processes, also known as tearing. Due to this reconnection, magnetic islands are created on surfaces at locations where q is resonant. On these flux surfaces, groups of islands form which correspond in the number of islands in the poloidal and toroidal directions with the poloidal and toroidal mode numbers of the resonance at that location.

One method of visualizing the changes in the magnetic topology is by using a Poincaré plot. The simplest approach to modelling the effects of RMPs on the plasma is to superpose the axisymmetric equilibrium field with the additional perturbation field. This is a vacuum approach as no plasma is considered, although the field produced by the toroidal plasma current is included. Knowing the total magnetic field

$\vec{B} = (B_R, B_\phi, B_Z)$, the field lines can be traced based on the equations

$$\frac{dR}{d\Phi} = R\frac{B_R}{B_\Phi}, \frac{dZ}{d\Phi} = R\frac{B_Z}{B_\Phi}. \quad (3)$$

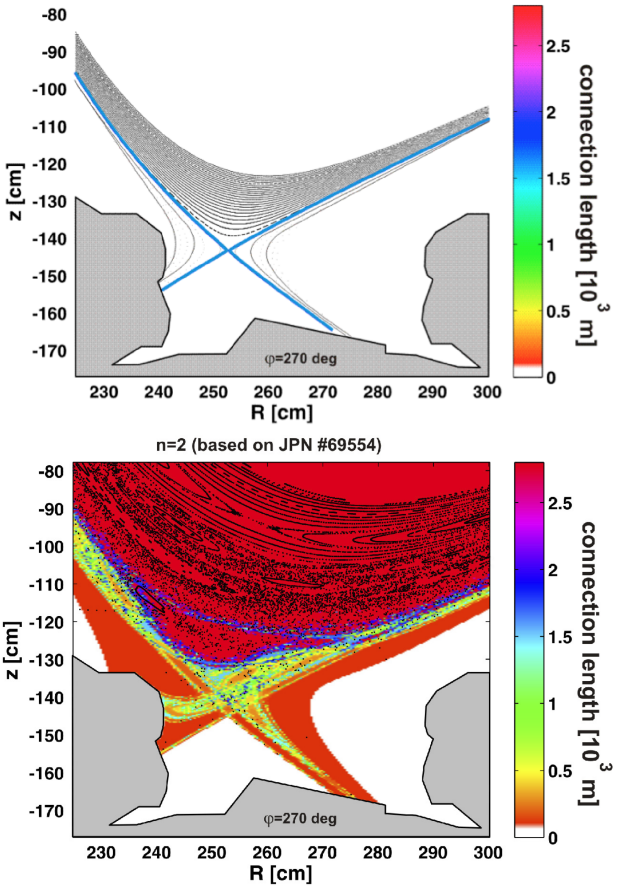

Figure 4: Poincaré plots of the separatrix topology combined with the contour plots of the connection length of the field lines with (upper) and without (lower) $n = 2$ EFCC perturbations with $I_{EFCC} = 32kAt$.

The crossing points of the field lines with the poloidal cross-section at a fixed toroidal angle Φ generate the Poincaré plot. Figure 4 (upper and lower) shows the modification of the magnetic topology when an $n = 2$ EFCC field was applied to a 2D poloidal divertor equilibrium. Here, the combined Poincaré plots of the stochastic magnetic field structures and the connection length of the perturbed field lines are calculated by the GOURDON field line tracing code [16] for an $n = 2$ EFCC configuration on JET. The calculation is based on an equilibrium reconstruction used for the calculation of the spectrum in figure 2 with the perturbation field superposed according to the vacuum approach [17]. Screening effects due to plasma rotation have been neglected. However, these initial results clearly exhibit the stochastic nature of the field line behaviour in the region around the X-point where the plasma rotation is low. The lobes of the manifolds step out, seen as a splitting of the strike point. The connection length of the perturbed field lines slightly inside the separatrix is a few $100m$, which is less than ~ 20 toroidal turns.

The plasma edge of magnetic confinement devices is of great interest in RMP physics. In that region, the effective perturbation (the perturbation field normalized to the toroidal field), is aimed to be highest in order to achieve a strong stochastization. Within the stochastic region, the radial transport is enhanced, which changes the plasma parameters [19, 20, 21, 22] and may explain experimental observations like the heat redistribution [23], modification of the edge electric field [24, 25] , and the control of edge instabilities [15, 26, 27].

III. 3D BOUNDARY PLASMA PHYSICS

Within the last decade, it has become clear that the magnetic topology of a plasma in a tokamak cannot be fully described by the simple vacuum approach. In particular, during plasma operation in H-mode, additional currents exist in the plasma or are created as a response of the plasma to the applied external RMP fields. Many studies [28, 29, 30, 31, 32] have shown that this plasma response needs to be considered in order to understand the ongoing processes in a tokamak plasma in the presence of RMPs. The two main effects discussed are RMP field screening and the 3D equilibrium effect in low- or moderate-beta plasmas. Resonant field amplification has to be considered in high-beta plasmas, in which the external kink mode naturally becomes unstable. In addition, particle drifts in H-mode operation appear to have a strong influence [33]. Different ideas for improving the vacuum approach are discussed [33, 34, 35] and new methods based on kinetic [36] and fluid modelling used [37, 38, 39]. All these improved modelling approaches show an impact on the magnetic topology in the edge and core regions leading to modified plasma transport.

A. Plasma rotation screening effect on the RMPs

Depending on the plasma parameters and RMP spectrum, the actual RMP field could be very different in rotating plasmas, where the generation of current perturbations on rational surfaces could prevent reconnection and island formation, leading to the effective screening of RMPs [36, 40]. The equilibrium radial electric field produces $\vec{E} \times \vec{B}$ rotation which, together with the diamagnetic electron rotation, is particularly important for RMP screening in the pedestal region [38, 41].

Generally, the screening effect increases for lower resistivity, stronger rotation and smaller RMP amplitude. For an H-mode plasma with a steep pressure gradient at the edge pedestal, RMP penetration typically only occurs in the narrow region near

the separatrix due to the higher resistivity. However, at certain plasma parameters and/or because of the non-linear evolution of the radial electric field due to RMPs, $\vec{E} \times \vec{B}$ perpendicular rotation can be compensated by the electron diamagnetic rotation, i.e. $(V_{\theta,\vec{E}\times\vec{B}} + V^*_{\theta,e} \sim 0)$. In this case, the RMP harmonic (n, m) penetrates locally and forms islands on the corresponding resonant surface $q = m/n$ [42].

B. 3D equilibrium with a stochastic boundary

Tokamaks are often considered to be two-dimensional and consequently, their equilibrium is treated by solving the Grad-Shafranov equation. In real devices, the toroidal field ripple, error fields due to coil misalignments and the deliberate application of RMPs lead to a three-dimensional problem. The addition of RMPs to an axisymmetric equilibrium perturbs the force balance

$$\nabla p \neq \vec{J} \times (\vec{B} + \vec{B}_{pert,vac}). \quad (4)$$

Here, p, $\vec{J}$ and $\vec{B}$ are the plasma pressure, current density and magnetic field in an axisymmetric equilibrium, and $\vec{B}_{pert,vac}$ is the 3D vacuum perturbation field. To study the effect of the deviations from axisymmetry on the equilibrium the application of complex numerical tools is necessary. To re-establish the force balance, a 3D equilibrium including an equilibrium response to the 3D perturbation fields is needed.

$$\nabla p + \nabla p_{res} = (\vec{J} + \vec{J}_{res}) \times (\vec{B} + \vec{B}_{pert,vac} + \vec{B}_{res}). \quad (5)$$

Here, p_{res}, $\vec{J}_{res}$ and $\vec{B}_{res}$ are the 3D plasma responses of pressure, current density and magnetic field to the applied perturbation fields.

Nowadays, a number of numerical codes for the calculation of 3D MHD equilibria are available (VMEC, PIES, HINT2, IPEC). Some assume nested flux surfaces (VMEC, IPEC), while others allow for magnetic islands (PIES, HINT2). On TEXTOR, the HINT2 code [43] is used to compute numerical 3D equilibria. The converged 3D equilibria are compared with the simple vacuum superposition assumption for the case with a DED current of $7.5kA/coil$. While the major structures are conserved in the HINT2 calculation, an additional ergodisation around the X-points of the major islands (e.g. the 3/2 island) appears. Furthermore, secondary structures appear in the islands, a feature already observed experimentally for 2/1 islands with the DED in 3/1 configuration [44]. This effect is caused by the modified Pfirsch-Schlüter current density distribution driven by the pressure gradient around the island. In figure 5 (a) and (b), connection length plots for an enlarged edge area are shown and indicate an increased island size in the HINT2 case. Furthermore, a statistical analysis shows an increase in short ($\leq 1000m$) and very long ($\approx 16000m$) field lines (see figure 5 (c)) in the HINT2 case. This indicates a shaper transition from the confined core to the vacuum region. It should be noted

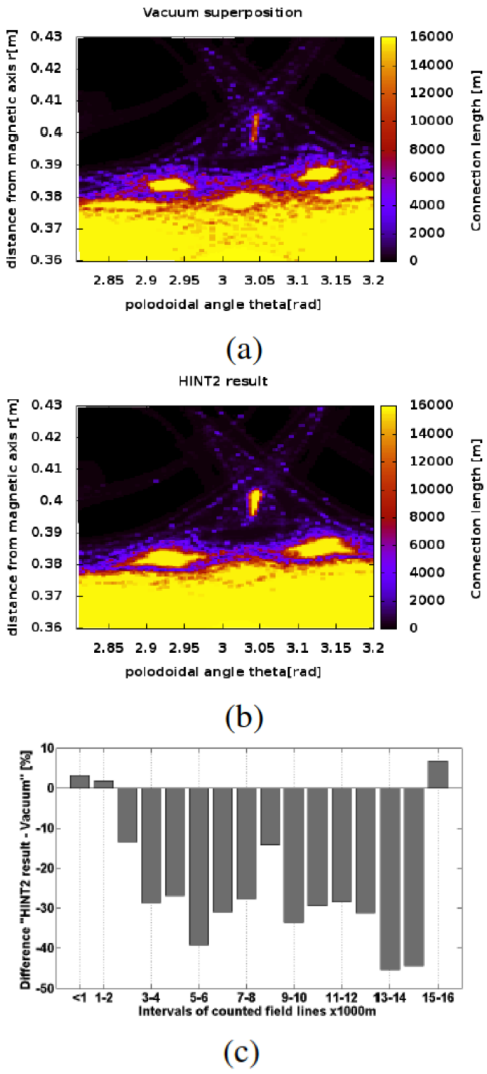

Figure 5: Connection length plots: (a) vacuum, (b) HINT2. (c) Difference in the number of field lines in specified length intervals: HINT2 result minus vacuum superposition in percent.

that the screening of the RMPs due to plasma rotation is not taken into account in the present HINT2 calculation.

C. Plasma transport in the stochastic boundary

A strong effect on the electron and thus heat transport is expected in a deep stochastic boundary layer ($\sigma_{ch} \gg 1$). The field line diffusion coefficient D_{FL}, and the electron heat diffusion coefficient can be described as :

$$\chi_e = D_{FL}\nu_{th}, D_{FL} = \sum_{m,n} \pi q R_0 |\frac{\delta B_{m,n}}{B_0}|^2. \quad (6)$$

Here, ν_{th} is the electron thermal velocity, $\delta B_{m,n}$ is the resonant component of the magnetic perturbation field. The electron heat transport in a stochastic boundary layer can be of the order of $10 - 100m^2s^{-1}$ over the perturbed edge and largely exceeds the usual anomalous transport $\sim 1m^2s^{-1}$ at the plasma edge.

Spin-up of the edge plasma rotation in the co-current direction and a change of the plasma edge electric field to a more positive value in the stochastic boundary layer have been observed in experiment [45]. This is due to the much larger electron mobility compared to the ion mobility implying an electron-retarding electric field in the plasma edge, which was previously dominated by ion losses due to their larger Larmor radius.

The effect of an additional radial diffusion on particle transport is difficult to analyse due to the coupling of the complicated transport regime to that of the physics of particle sources, namely neutral penetration. On JET, in a low- or a moderate-collisionality regime (electron collisionality at the pedestal, $\nu^*_{ped,e} \leq 1$), the electron density at the pedestal top decreased by $\sim 20\%$, the so-called density pump-out [46], during the application of an $n = 1$ field, while the pedestal electron temperature increased, keeping the pedestal pressure almost constant. However, the pedestal pressure gradient obtained from the derivative of the fitted curve shows that the maximum pressure gradient in the profile is decreased by 20% during the application of the $n = 1$ field, and the edge pressure barrier is 20% wider [47]. This is an effect mostly ascribable to the strong decrease in the n_e pedestal height with an almost unvaried width. In a high-collisionality regime ($\nu^*_{ped,e} > 1$), the effect of RMPs on the pedestal particle and heat transport is not clearly observed. [51].

Compensation of the density pump-out has been also investigated on JET using either gas fuelling or pellet injection in low-triangularity H-mode plasmas [17, 49, 50]. Although the ELM frequency stays high with $n = 1$ fields, no recovery of stored energy is observed. An optimized fuelling rate for compensating the density pump-out effect has been identified, and it depends on the plasma configuration.

D. Effects of a stochastic boundary layer on plasma-wall interaction

In the edge transport model, the transport of power in the stochastic layer has been treated as a diffusive process [55], which gives a significantly enlarged effective cross-field transport for the electron energy. As a result, a widening of the contact zone between plasma and wall has been predicted[56]. Experimental results from different devices [23, 57] have proved that the heat and particle deposition patterns are strongly structured.

The resulting heat deposition pattern reflects the complicated structure of the perturbed volume. It has been shown in [52] that the connection length and the radial penetration of the magnetic field lines defines the amount of power deposited on the target structures. The maximum of the heat flux density corresponds to the field lines with long connection length; however, those with shallow penetration seem to be strongly affected by the collisionality, in contrast to the field lines with deep penetration, which connect the outermost existing island chain to the divertor surface. For a proper analysis of such a complicated topology, inevitably one needs 3D transport codes, which could describe such a variety of magnetic field lines.

As an example, splitting of the outer strike point (SP), appearing as multiple peaks in the ELM heat flux profile along the outer divertor plate, has been measured by a fast IR camera during the application of $n = 2$ fields on JET with the ITER-like wall (ILW) as shown in figure 6. These multiple peaks in the heat flux profile are observed only during a mitigated ELM crash when a certain I_{EFCC} threshold is reached. The preliminary results indicate that this I_{EFCC} threshold for the appearance of splitting of the outer SP during the ELM crash is at a similar level to that occurring for the saturation effect of the plasma response. Similar findings of strike point splitting have been reported on DIII-D in the presence of $n = 3$ RMP fields [53].

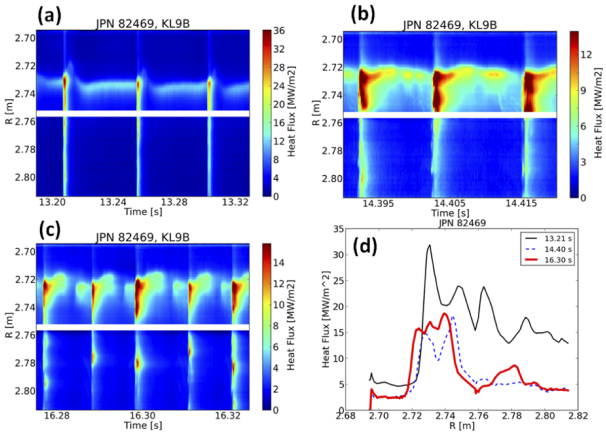

Figure 6: Extended time traces of the heat flux distribution on the outer divertor plate in the phases (upper left) without $n = 2$ field, (upper right) with $I_{EFCC} = 44$ kA and (lower left) with $I_{EFCC} = 88$ kA. (Lower right) ELM peak heat flux profiles along the outer divertor. From reference [51]

.

IV. ELM CONTROL USING RMP

Active control of ELMs by RMP fields offers an attractive method for next-generation tokamaks, e.g. ITER. The results obtained from the DIII-D, JET, MAST, KSTAR, AUG and NSTX tokamaks have shown that magnetic field perturbations can either completely suppress ELMs [15], trigger small ELMs during ELM-free periods, or affect the frequency and size of the type-I ELMs in a controllable way, preserving good global energy confinement [14].

A. Type-I ELM suppression with RMPs

The first successful demonstration of the ELM suppression technique was reported from DIII-D [15], where the in-vessel coils (I-coils) were employed. The I-coils consist of 12 single-turn loops, six above and six below the midplane (up-down symmetric) mounted on the low-field side of the vessel. For the ELM suppression experiments, the upper and lower loops are operated with either the same current polarities (even parity) or opposite current polarities (odd parity), and induce a static perturbation field with a toroidal mode number $n = 3$.

On DIII-D, the experimental results show that the effectiveness of ELM suppression with $n = 3$ fields depends on q_{95}. In low collisionality ($\nu^*_{ped,e} \leq 0.2$) H-mode plasmas, ELM suppression without small intermittent events is obtained in a narrow q_{95} window ranging from 3.5 to 3.9 with an even parity $n = 3$ field and ~ 7.2 with an odd parity $n = 3$ field. Outside this q_{95} range, type-I ELMs are mitigated (ELM frequency increased and ELM size decreased) by the applied $n = 3$ fields. These results indicate a resonant condition on the amplitude of RMPs for ELM suppression.

B. Type-I ELM mitigation with RMPs

Active control of type-I ELMs by the application of static $n = 1$ or 2 perturbation fields has been developed for more ITER-relevant configurations and parameters in a wide operational space of plasma triangularity (δ_U up to 0.45), q_{95} $(4.8 - 3.0)$ and beta (β_N up to 3.0) on JET [14, 48, 49, 17]. The first results of ELM mitigation with $n = 2$ fields on JET demonstrate that the frequency of ELMs can be increased by a factor of $\sim 4-5$, limited by the available EFCC coil current. A wide operational window of q_{95} has also been obtained for ELM mitigation with $n = 2$ fields. During the application of the $n = 1, 2$ fields, a reduction in the ELM size (ΔW_{ELM}) and ELM peak heat flux on the divertor target by roughly the same factor as the increase in the ELM frequency has been observed. The reduction in heat flux is mainly due to the drop of particle flux rather than a change of the electron temperature. A modest drop (a few per cent) in the total stored energy has been observed during the ELM control phase with the EFCCs. However, when normalized to the $IPB98(y, 2)$ scaling, the confinement time shows almost no reduction.

Recently, mitigation of type-I ELMs was observed with an $n = 2$ field on JET with the ITER-like wall (ILW) [51]. A strong mitigation of type-I ELMs was observed when an $n = 2$ field was applied in high-collisionality ($\nu^*_{ped,e} = 2.0$) H-mode plasmas. No density pump-out effect was observed in the high-collisionality case, but was observed in the low-collisionality case. In the moderate-collisionality type-I ELMy H-mode plasmas with the ILW wall, a saturation effect of ELM mitigation and clear pre-ELM structures were observed on the outer divertor plate during the application of $n = 2$ fields, depending on q_{95}[51, 54].

V. SUMMARY AND OPEN QUESTIONS

Regarding on the control of plasma transport in the boundary zones, two conflicting issues have to be balanced. On one hand, to achieve a homogenization of the power deposition on target plates and reduce the peak heat flux on the divertor or the limiter, a high cross field transport level is required in the SOL. On the other hand, to keep a high fusion gain, good confinement with the edge plasma transport barrier (H-mode), is required. One attractive idea for broadening the SOL and distributing the particle and heat fluxes more evenly and over a larger surface is to soften the edge of the magnetic cage by the formation of a stochastic boundary with the application of external magnetic perturbations.

In tokamaks, non-axisymmetric magnetic perturbations, which change the magnetic topology, have been applied on the majority of contemporary large-scale tokamaks to control plasma edge stability and transport. Recent research has highlighted the significance of the role that stochasticity and 3D magnetic topology also play in this fundamentally 2D concept. Their influence can be seen in transport and energy confinement, in the control of various MHD instabilities, most notably ELMs, which expel considerable amounts of energy from the plasma and pose a risk of damaging plasma-facing components in ITER and other next-generation fusion devices.

RMP ELM suppression/control has shown very promising results up to now, although the physics mechanism is not well understood as yet. Future joint experiments from different devices (DIII-D, JET, MAST, NSTX, AUG, TCV, KSTAR and EAST) will help us to understand ELM suppression physics and provide support for ITER.

To date, many attempts to explain ELM suppression have focused on the idea that the edge thermal and particle losses are enhanced due to the formation of an outer 'ergodic' zone with RMP fields. This 'ergodic' boundary would reduce the edge pressure gradients, and thus stabilize the peeling-ballooning modes thought to underlie ELM formation [15], [37]. This mechanism is mainly supported by two experimental results from DIII-D: i) splitting of the inner strike-point observed during the RMP ELM suppression phase; and ii) spin-up of the edge plasma rotation in the co-current direction and a change of the plasma edge electric field to a more positive value due to larger losses of electrons than ions with an ergodic boundary. However, either bulk plasma or diamagnetic rotation can screen the RMP fields from the resonant magnetic flux surfaces. Many calculations of the Chirikov parameter or overlapping of resonant magnetic islands employ a vacuum assumption, which

neglects the plasma response (rotational screening effect and equilibrium effect).

Although the mechanism of ELM control with RMPs is not yet fully understood, it has been examined in a wide operational window in many different devices. Further optimisation of the magnetic perturbation with less reduction of the plasma performance, and an understanding of the underlying physics are essential for future investigations.

In addition, the existence of these stochastic and 3D magnetic topology effects brings tokamak and stellarator physics closer together, and a holistic approach to studying them provides the most promising path to making good progress. Understanding these effects is essential for the success of future fusion devices, and they represent a hot topic in current fusion research. Furthermore, reversed field pinches offer access to these topics with unique features such as the bifurcation into self-generated 3D equilibria and multi-mode unstable plasma conditions with a high degree of magnetic field stochasticity.

REFERENCES

1. "ITER Physics Basis", *Nucl. Fusion* **39** 2137 (1999)
2. F. Wagner et al., "Regime of Improved Confinement and High Beta in Neutral-Beam-Heated Divertor Discharges of the ASDEX Tokamak", *Phys. Rev. Lett.*, **49**, 1408 (1982).
3. T. Eich, et al., "Inter-ELM Power Decay Length for JET and ASDEX Upgrade: Measurement and Comparison with Heuristic Drift-Based Model", *Phys. Rev. Lett.*, **107**, 215001 (2011).
4. Loarte A, et al., "ELM energy and particle losses and their extrapolation to burning plasma experiments", *J. Nucl. Mater.*, **313-316** 962 (2003)
5. A. Einstein, "Über die von der molekularkinetischen Theorie der Wärme geforderte Bewegung von in ruhenden Flüssigkeiten suspendierten Teilchen", *Ann. Phys.*, **17** 549-560 (1905).
6. J. Klafter and M. Sokolov, "Anomalous diffusion spreads its wings", *Physics World*, **18** 29-32 (2005).
7. R. Kubo, "Statistical-mechanical theory of irreversible processes: I. General theory and simple applications to magnetic and conduction problems", *J. Phys. Soc. Japan*, **12** 570 (1957).
8. B. V. Chirikov, "A universal instability of many-dimensional oscillator systems", *Phys. Rep.* **52** 263?379 (1979).
9. G. M. Zaslavsky, "Chaos, fractional kinetics, and anomalous transport", *Phys. Rep.* **371** 461?580 (2002).
10. G. M. Zaslavsky, "Hamiltonian Chaos and Fractional Dynamics", *Oxford: Oxford University Press* (2005)
11. S. Chandrasekhar, "Stochastic problems in physics and astronomy", *Rev. Mod. Phys.* **15** 1?89 (1943)
12. R. Balescu, "Aspects of Anomalous Transport in Plasmas" *Bristol: Institute of Physics Publishing* (2005)
13. Y. Liang, "Overview of edge-localized mode control in tokamak plasmas", *Fusion Science and Technology* **59**, 586 (2011).
14. Y. Liang, et al., "Active control of type-I edge-localized modes with n=1 perturbation fields in the JET tokamak", *Phys. Rev. Lett.*, **98** 265004 (2007)
15. T. E. Evans, et al., "Edge stability and transport control with resonant magnetic perturbations in collisionless tokamak plasmas", *Nature Phys.*, **2** 419 (2006)
16. C. Gourdon, "Programme optimise de calculs numeriques dans les configurations magnetiques toroidales", *CEN Fontenay aux Roses* (1970)
17. Y. Liang, et al., "Active control of type-I edge localized modes with n = 1 and n = 2 fields on JET", *Nuclear Fusion* **50**, 025013 (2010).
18. Y. Liang, et al., "Magnetic Topology Changes Induced by Lower Hybrid Waves and their Profound Effect on Edge-Localized Modes in the EAST Tokamak", *Phys. Rev. Lett.*, **110** 235002 (2013)
19. T. Stix. "Plasma transport across a braided magnetic field", *Nuclear Fusion*, **18**, 353?358 (1978).
20. H. Wobig and R. H. Fowler, "The effect of magnetic surface destruction on test particle diffusion in the Wendelstein VII-A stellarator", *Plasma Physics and Controlled Fusion* **30**, 721 (1988).
21. T. Eich, D. Reiser and K. Finken, "Two dimensional modelling approach to transport properties of the TEXTOR-DED laminar zone", *Nuclear Fusion* **40**, 1757 (2000).
22. A. Wingen, S. Abdullaev, K. Finken, M. Jakubowski and K. Spatschek, "Influence of stochastic magnetic fields on relativistic electrons", *Nuclear Fusion* **46**, 941 (2006).
23. M. W. Jakubowski, S. Abdullaev, K. Finken and the TEXTOR Team, "Modelling of the magnetic field structures and first measurements of heat fluxes for TEXTOR-DED operation", *Nuclear Fusion* **44**, S1 (2004).

24. S. Jachmich, P. Peleman, M. Van Schoor, Y. Xu, M. Jakubowski, M. Lehnen, B. Schweer and R. Weynants, "First Mach probe measurements of rotation, electric field and particle transport in the DED-ergodized edge plasma of TEXTOR", In: *Proceeding of the 33rd EPS Conference on Plasma Physics*, **O3.014** (2006)

25. A. Wingen and K. Spatschek, "Influence of different DED base mode configurations on the radial electric field at the plasma edge of TEXTOR", *Nuclear Fusion* **50**, 034009 (2010).

26. O. Schmitz et al., "Aspects of three dimensional transport for ELM control experiments in ITER-similar shape plasmas at low collisionality in DIII-D", *Plasma Physics and Controlled Fusion* **50**, 124029 (2008).

27. Y. Liang, C. G. Gimblett, P. K. Browning, P. Devoy, H. R. Koslowski, S. Jachmich, Y. Sun and C. Wiegmann, "Multiresonance Effect in Type-I Edge-Localized Mode Control With Low n Fields on JET", *Physical Review Letters* **105**, 065001 (2010).

28. T. E. Evans, I. Joseph, R. Moyer, M. Fenstermacher, C. Lasnier and L. Yan. "Experimental and numerical studies of separatrix splitting and magnetic footprints in DIII-D", *Journal of Nuclear Materials* **363-365**, 570-574 (2007).

29. E. Nardon et al. "Strike-point splitting induced by external magnetic perturbations: Observations on JET and MAST and associated modelling", *Journal of Nuclear Materials* **415**, S914-S917 (2011).

30. A. Kirk et al. "Magnetic perturbation experiments on MAST L- and H-mode plasmas using internal coils", *Plasma Physics and Controlled Fusion* **53**, 065011 (2011).

31. Y. Yang, Y. Liang, Y. Sun, T. Zhang, J. Pearson, Y. Xu and TEXTOR Team. "Experimental observations of plasma edge magnetic field response to resonant magnetic perturbation on the TEXTOR Tokamak." *Nuclear Fusion* **52**, 074014 (2012).

32. P. Denner, Y. Liang, Y. Yang, M. Rack, L. Zeng, J. Pearson, Y. Xu and the TEXTOR team. "Local measurements of screening currents driven by applied RMPs on TEXTOR". *Nuclear Fusion* **54** (2014).

33. A. Wingen, O. Schmitz, T. E. Evans and K. H. Spatschek. "Heat flux modeling using ion drift effects in DIII-D H-mode plasmas with resonant magnetic perturbations", *Physics of Plasmas*, **21**, 012509 (2014).

34. P. Cahyna and E. Nardon. "Model for screening of resonant magnetic perturbations by plasma in a realistic tokamak geometry and its impact on divertor strike points", *Journal of Nuclear Materials* **415**, S927 ?S931 (2011).

35. H. Frerichs, D. Reiter, O. Schmitz, P. Cahyna, T. E. Evans, Y. Feng and E. Nardon. "Impact of screening of resonant magnetic perturbations in three dimensional edge plasma transport simulations for DIII-D", *Physics of Plasmas* **19**, 052507 (2012).

36. M. F. Heyn, I. B. Ivanov, S. V. Kasilov, W. Kernbichler, I. Joseph, R. A. Moyer and A. M. Runov. "Kinetic estimate of the shielding of resonant magnetic field perturbations by the plasma in DIII-D", *Nuclear Fusion*, **48**, 024005 (2008).

37. M. Bécoulet et al. "Physics of penetration of resonant magnetic perturbations used for Type I edge localized modes suppression in tokamaks.", *Nuclear Fusion* **49**, 085011 (2009).

38. E. Nardon, P. Tamain, M. Bcoulet, G. Huysmans and F. Waelbroeck. "Quasi-linear MHD modelling of H-mode plasma response to resonant magnetic perturbations", *Nuclear Fusion* **50**, 034002 (2010).

39. A. Wingen, N. M. Ferraro, M. W. Shafer, E. A. Unterberg, T. E. Evens, D. L. Hillis and P. B. Snyder. "Impact of plasma response on plasma displacements in DIII-D during application of external 3D perturbations", *Nuclear Fusion* **54** (2014).

40. R. Fitzpatrick, "Bifurcated states of a rotating tokamak plasma in the presence of a static error-field", *Phys. Plasmas* **5** 3325 (1998)

41. D. Reiser D. and D. Chandra, "Plasma currents induced by resonant magnetic field perturbations in tokamaks", *Phys. Plasmas* **16** 042317 (2009)

42. M. Bécoulet, et al., "Screening of resonant magnetic perturbations by flows in tokamaks", *Nuclear Fusion*, **52** 054003 (2012)

43. Y. Suzuki, et al., "Development and application of HINT2 to helical system plasmas", *Nuclear Fusion*, **46** L19-L24 (2006)

44. Y. Liang, et al., "Observations of secondary structures after collapse events occurring at the q = 2 magnetic surface in the TEXTOR tokamak", *Nuclear Fusion*, **47** L21-L25 (2007)

45. K. H. Finken, et al., "Toroidal plasma rotation induced by the Dynamic Ergodic Divertor in the TEXTOR tokamak",*Phys. Rev. Lett.* **94** 015003 (2005)

46. J. C. Vallet et al., "Stabilization of tokamak Ohmic discharges at the density limit by means of the ergodic divertor", *Phys. Rev. Lett.* **67** 2662 (1991)

47. A. Alfier et al., "Edge T-e and n(e) profiles during type-I ELM mitigation experiments with perturbation fields on JET" *Nucl. Fusion* **48** 115006 (2008)

48. Y. Liang, et al., "Active control of type-I edge localized modes on JET", *Plasma Phys. Control. Fusion* **49** B581 (2007)

49. Y. Liang, et al., "Active control of edge localized modes with a low n perturbation fields in the JET tokamak", *J. Nucl. Mater.* **390-91** 733-739 (2009)

50. Y. Liang, et al., "Overview of ELM Control by Low n Magnetic Perturbations on JET", *Plasma and Fusion Research*, **5**, S2018 (2010)

51. Y. Liang, et al., "Mitigation of type-I ELMs with n=2 fields on JET with ITER-like wall", *Nucl. Fusion* **48** 115006 (2013)

52. M. W. Jakubowski, et al., "Observation of the heteroclinic tangles in the heat flux pattern of the ergodic divertor at TEXTOR", *J. Nucl. Mater.* **363** 371-376 (2007)

53. M. W. Jakubowski et al., "Overview of the results on divertor heat loads in RMP controlled H-mode plasmas on DIII-D", *Nucl. Fusion* **49**, 095013 (2009).

54. M. Rack, et al., "Findings of pre-ELM structures through the observation of divertor heat load patterns at JET with applied n=2 perturbation fields", *Nucl. Fusion* **54**, 072004 (2014).

55. A. B. Rechester and M.N. Rosenbluth, "Electron Heat Transport in a Tokamak with Destroyed Magnetic Surfaces", *Phys. Rev. Lett.* **40** 38 (1978)

56. A. V. Nedospasov and M.Z. Tokar, "Conception of divertorless tokamak reactor with turbulent plasma blanket", *J. Nucl. Mater.* **93-94** 248 (1980)

57. A. Grosman, P. Ghendrih, B. Meslin and D. Guilhem, "Power and particle flux to the neutraliser plates of the Tore Supra ergodic divertor modules", *J. Nucl. Mater.* **241-243** 532 (1997)